

Accepted Manuscript

Moisture content and chloride ion effect on the corrosion behavior of fitting brass (gate valves) used as a connection of PVC's conduits in aggressive sandy soil

M. Galai , J. choucri , Y. Hassani , H. Benqlilou , I. Mansouri ,
B. Ouakki , M. Ebn Touhami , C. Monticelli , F. Zucchi

PII: S2405-8300(18)30048-X
DOI: <https://doi.org/10.1016/j.cdc.2018.11.013>
Reference: CDC 171



To appear in: *Chemical Data Collections*

Received date: 4 March 2018
Revised date: 29 November 2018
Accepted date: 29 November 2018

Please cite this article as: M. Galai , J. choucri , Y. Hassani , H. Benqlilou , I. Mansouri , B. Ouakki , M. Ebn Touhami , C. Monticelli , F. Zucchi , Moisture content and chloride ion effect on the corrosion behavior of fitting brass (gate valves) used as a connection of PVC's conduits in aggressive sandy soil, *Chemical Data Collections* (2018), doi: <https://doi.org/10.1016/j.cdc.2018.11.013>

This is a PDF file of an unedited manuscript that has been accepted for publication. As a service to our customers we are providing this early version of the manuscript. The manuscript will undergo copyediting, typesetting, and review of the resulting proof before it is published in its final form. Please note that during the production process errors may be discovered which could affect the content, and all legal disclaimers that apply to the journal pertain.

Chemical Data Collections article template

Title:Moisture content and chloride ion effect on the corrosion behavior of fitting brass (gate valves) used as a connection of PVC's conduits in aggressive sandy soil

Authors:M.Galai^{1,*}, J.choucri^{1,2}, Y. Hassani¹, H. Benqlilou³, I.Mansouri³, B. Ouakki⁴, M. Ebn Touhami^{1,*}, C. Monticelli², F. Zucchi²

Affiliations:

¹ Laboratory of Materials Engineering and Environment: Modeling and Application, Faculty of Science, University Ibn Tofail BP. 133-14000, Kenitra, Morocco.

² Centro di Studi sulla Corrosione e Metallurgia "Aldo Daccò" Via Saragat, 4/a - 44122 Ferrara –Italia.

³ International Institute for Water and Sanitation (IEA), National office of Electricity and the Potable Water, Morocco.

⁴ Ecole Nationale Supérieure des Mines de Rabat, Morocco

Contact email:galaimouhsine@gmail.com / m.ebntouhami@gmail.com

Abstract

The corrosion of four brasses EC1 and EC2 of ($\alpha+\beta$) brass type while EC3 and EC4 are of α -brass type in the aggressive sandy soil collected in a suburban area of Essouira Morocco was studied. The original soil was characterized, and modified by adding the chloride ions or by increasing its moisture content. The corrosion behavior of these brasses in soil was investigated at ambient temperature using various electrochemical methods. The different alloy surfaces were examined by scanning electron microscopy, whereas the chemical composition was determined by EDS analysis. EIS measurements indicated that the corrosion rate of all brasses series increases with increasing the moisture content of the studied soil up to critical limit (30 wt%), then it starts to decrease with further increase of moisture content. It was found that the chemical composition of brass influences the corrosion rate, especially the presence of iron, Nickel and Arsenic. Furthermore, EC3 is always the most resistant among the other alloy even in a very aggressive environment containing the chloride ions with a concentration of 2%.

Keywords

Corrosion, Brass, Soil, Moisture content, Chloride ions.

Specifications Table

Subject area	<i>Physical Chemistry, Chemical Engineering, Corrosion science.</i>
Compounds	NA
Data category	<i>Potentiodynamic polarization (PDP), Electrochemical impedance spectroscopy (EIS), Scanning electron microscopy SEM, EDS analysis.</i>
Data acquisition format	<i>Potentiodynamic polarization (PDP), Electrochemical impedance spectroscopy (EIS), Scanning electron microscopy SEM, EDS analysis.</i>
Data type	<i>Filtered, analyzed, simulated.</i>
Procedure	<i>The original soil was characterized, and modified by adding chloride ions or by increasing its moisture content. The corrosion behavior of these brasses in soil was investigated at ambient temperature ($25\pm 2^\circ\text{C}$) using various electrochemical methods like potentiodynamic polarization (PDP), and electrochemical impedance spectroscopy (EIS). The different alloy surfaces were examined by scanning electron microscopy SEM, whereas the chemical composition was determined by EDS analysis. EIS measurements indicated that the corrosion rate of all brass series increased with increasing the moisture content of the studied soil up to a critical limit (30 wt%), but it started to decrease with an additional rise in the moisture content.</i>
Data accessibility	Data included in the article.

1-Rationale

Brass is defined as a metallic alloy which is mostly made of both zinc and copper. Typically, brass has a golden coloration like copper, which prevents from corrosion, while it maintains copper's malleability. As a result, it is often observed at the plumbing and sanitary fittings of houses, which are always affected by corrosive environments [1]. Both of zinc and copper proportions can be changed to make several series of brasses characterized by various properties including strength, wear resistance, hardness, color, ductility, electrical, thermal, antimicrobial conductivity, machinability, and corrosive resistance [2]. These various kinds of brass respond to corrosion effect in different ways and in different mediums.

The brass dezincification is much closed to an alloy structure which is controlled by composition. It is also noticed that the resistance to this dezincification increases with copper, which enters the composition of brass, but the relationship is not linear. Many positive changes in performance had occurred when the structure varied from all-beta to $(\alpha+\beta)$ duplex and from duplex to all-alpha phase. Alloys containing less than 15% Zn rarely dezincify [3, 4].

Generally, there are three different methods of preventing or minimizing dezincification. Firstly, α -brass can be used in place of $(\alpha+\beta)$ brasses which are more susceptible to dezincification. The reason for this increased susceptibility is that in an electrolyte the zinc-rich β -phase is anodic with respect to the more copper-rich α -phase. The second method, derived from the Cu-Zn phase diagram [5], is to thermally treat two-phase brasses (Zn, 39%) to transform them to the single α -phase. This can be conducted by heating

from 400°C to 600°C with subsequent quenching to room temperature [6,7]. But this treatment renders the alloy less susceptible to dealloying and the thermal process makes the method non-cost effective. The third and presently most economic method to minimize dezincification is to add low levels of suitable elements to the alloy. These elements include arsenic [8, 9], antimony [10], boron [11], phosphorus [12], tin and aluminum [13]. Among these, arsenic has attracted the most interest because it is highly effective in preventing dezincification of α -brasses [6-8].

The effect of the soil composition on the corrosive resistance of buried metallic substances and corrosion products nature are formed in many industrial applications and in archaeological surveys of metallic finds [14-17]. The modifications in the soil characteristics can emerge from agricultural practices like fertilization where chemicals are accidentally spilled into the soil (acids or strong bases), acid rains, seawater intrusion etc...

The present work investigates the effect of both soil humidity content and chloride ions on the corrosion behavior of two materials; α -brass and two ($\alpha+\beta$) brasses alloys in soils from Essaouira city of Morocco (sandy soil type) at ambient temperature ($25\pm 2^\circ\text{C}$). Several authors [18-23] have investigated the influence of soil moisture including the influence of chloride ions on the corrosion of copper. Moreover, many studies have been investigated in order to study steel corrosion [24-27].

The plumbing system studied is shown in Figure 1.

2-Procedure

2.1. Materials and Methods

2.1. Materials

2.1.1. Soil sample preparation

A fraction of the soil collected in a suburban area of Essaouira, in Morocco, was dried at 105°C for 24 h and then left in the desiccator. The preparation of soil samples and their analysis were performed following procedures described in previous studies [28].

Table 1 gives the elements concentrations and the texture of the original soil sample (S1) and the studied soil materials which contains 13.6 % silt, 8.3% clay and 78.1% sand. These percentages can classify the studied soil as a sandy type.

The original soil sample (S1) was modified by adding 2% of NaCl. The procedure used for the preparation of the modified soil samples and their identification is given in Table 2. The volume of demineralized water was added to the weighted dried soil, and it was calculated in order to

give a relative humidity (RH) of 20%, 30% and 40% (samples S2, S3 and S4). The sample (S5) was prepared so that the added solution contains 2% of NaCl.

In addition, the electrochemical cell which was specifically designed for this study is represented in (Fig. 2) according to the literature [29].

Each soil sample was compacted manually in the electrochemical cell by applying a Proctor Compactor that consists of 3 kg of soil which is dropped from a height of 150 mm. The atmosphere inside the cell was constantly renewed via a flow of reconstituted air (80% of N₂ and 20 % of O₂) which circulated on the soil surface in the upper part of the cell

2.1.2. Composition of various brasses

Various types of brass alloys under investigation were classified in two types: α -brass and $\alpha+\beta$ brass. The chemical composition of these alloys is shown in Table 3. The chemical composition analysis is performed by optical emission spectrometer (OES).

The working electrode consists of a piece of brass wrapped by copper conductor wires tightly except for the top and bottom faces, and then covered by epoxy resin entirely except for an area of 0.78 cm² exposed to the soil. The coupons of brass were polished with emery paper (up to 1200 grade), washed by the deionized water, degreased by alcohol, and then dried naturally, respectively.

2.2. Electrochemical methods

2.2.1. Electrochemical impedance spectroscopy

Electrochemical impedance spectroscopy (EIS) measurements were performed using a transfer function analyzer (VoltaLab PGZ100) frequency response analyzer in a frequency range from 100 kHz to 10 mHz with 10 points per decade. The EIS diagrams were exposed in Nyquist representation. Then, the results were modeled through an equivalent electrical circuit using Boukamp program [30].

2.2.2. Polarization tests

The counter electrode was a stainless steel plate of large surface area and the reference electrodes were copper–copper sulphate electrodes Cu/CuSO₄ (+0.316 V/SHE at 25°C) which were commonly used in the field. In the following parts of this article, all used potentials were reported versus the reference electrode employed.

In addition, the working electrode was immersed in the soil during 21 days until a steady state open circuit potential (E_{ocp}) was obtained. The steady-state polarization curves were recorded potentiodynamically using a Volta Lab PGZ 100 and controlled by a personal computer. The cathodic polarization curve was recorded by polarization from (E_{ocp}) to negative direction (-1500 mV/Cu/CuSO₄) under potentiodynamic conditions corresponding to 1mV.s⁻¹ (scan rate). Then, the anodic polarization curve was recorded by polarization from (E_{ocp}) to positive direction (1200mV/ Cu/CuSO₄) under the same conditions as said before. The corrosion kinetic parameters were re-evaluated using the non-linear least squares method and applying equation Eq. (1) using Origin software. Nonetheless, for this calculation, the potential range applied was limited to ± 0.100 V next to E_{corr} , and a significant systematic divergence was noticed for both cathodic and anodic branches.

$$i = i_a + i_b = i_{corr} \times \{ \exp[b_a \times (E - E_{corr})] - \exp[b_c \times (E - E_{corr})] \}$$

Where i_{corr} (corrosion current density (A cm⁻²)) and b_a and b_c (the Tafel constants of anodic and cathodic reactions (V⁻¹) respectively), these constants are attached to the Tafel slopes β (V/dec) in usual logarithmic scale which is given by the following equation:

$$\beta = \frac{\ln(10)}{b} = \frac{2.303}{b}$$

2.3 Scanning electron microscopy (SEM)

The scanning electron microscopy (SEM) and the energy dispersive spectroscopy (EDS) studies were performed using a scanning electron microscope (SEM; JOEL JSM-5500). The elemental SEM-EDX analysis were carried out on the micro-analytical system LINK AN 10 000 operating in secondary and backscattered mode with acceleration voltage of 25 kV at extension 90-5500.

3. Data, value and validation

3.1. Influence of moisture on corrosion resistance

EIS was used to study the effect of moisture content of the sandy soil on the electrochemical behavior of two series of brass devices (α -brass and $\alpha+\beta$ -brass) used as a support fittings which are suitable for connecting domestic service lines at ambient temperature ($25 \pm 2^\circ\text{C}$). Figure

3 displays the variation in the measured electrochemical impedance (Nyquist plot) as a function of moisture content of Essaouira soil.

EIS data interpretation relies commonly on the development of equivalent circuits for modeling the metal/electrolyte (in the current case brass/soil) interface. To simulate the experimental EIS diagrams, various equivalent circuits were applied using a Bouckamp program.

Two equivalent circuits were obtained: one of them corresponds to the brass corrosion in Essaouira soil (Fig. 4a) at 14% moisture content, while the other one was for the corrosion of brass in the same soil for other moisture content 20%, 30% and 40% (Fig. 4b).

As can be shown in Fig. 13, the capacitor was substituted by a constant phase element, which indicates the presence of a dissimilar frequency response. The CPE impedance is known as [31];

$$Z_{CPE}(\omega) = Q^{-1}(j\omega)^{-n}$$

Where Q is a constant in $\Omega \cdot \text{cm}^{-2} \cdot \text{s}^n$, ω dimensions is the angular frequency in rad s^{-1} and n is the CPE exponent with $-1 < n < 1$. Z_{CPE} can represent an inductance ($n = -1$), a Warburg impedance ($n = 0.5$), a capacitance ($n = 1$), or a resistance ($n = 0$). However, the following elements form the suggested equivalent circuits:

R_s : oil resistance.

R_f : film resistance.

R_{ct} : the charge transfer resistance.

n_f and n_i : represent a depress feature in the Nyquist diagrams

Q_f and Q_i are the constant phase elements.

The same elements are used for the equivalent circuit (fig. 4.a) but with the addition of the Warburg coefficient S . The Nyquist curves corresponding to corrosion of the studied samples after 21 days of immersion in sandy soil of Essaouira versus moisture content are presented in figure 3. All the recorded Nyquist plots which correspond to the studied brasses with 20%, 30% and 40% of moisture content have shown a clear capacitive loop at high frequency, capacitive arc at intermediate frequency, and Warburg diffusive impedance at low frequency. However, the Nyquist plots which represent brasses with 14% of moisture content contain a capacitive loop at high frequency, capacitive loop at low frequency. It is also observed that there was a

similarity between all obtained plots, such behavioral characteristics for soil corrosion is a result of the low electrical conductivity and the higher ground impedance for "dispersion effect" [32]. In the soil corrosion, the generation of a "dispersion effect" due to the adhesion of the corrosion products with the soil particles to the surface of the metal electrode, modifies its state.

Table 3 represents the estimated electrochemical impedance parameters for all brass series corrosion in the studied soils with different moisture contents. The optimized values for polarization resistance R_p of all systems are also listed in Table 3. The (R_p) is calculated by using the following equation:

$$R_p = R_f + R_{ct} + R_s$$

The results mentioned in this Table can be explained as follows. It was found that the soil resistance (R_s) depends on the content of soil moisture. The increase of moisture content decreases the (R_s) value for the studied soil. The electrolytic performance of soils is based on the amount of soluble salts dissolved in the wet soil. Therefore, the increase in soil moisture can be related to the increase in the amount of soluble salts in the soil solution, which causes a decrease in soil resistance (R_s). This result was confirmed by Robain et al., Ozcep et al. and Ehteram A. Noor and others [33-35].

The evolution of fitted parameters for the alloys (brass devices) in Essaouira soil is presented in Table.4. According to the results, the parameter data was obtained. It was found that at all the moisture content, the (R_p) values of the both α -brass and ($\alpha+\beta$) brass in the studied soil respect the following order: EC3 > EC2 > EC1 > EC4.

Moreover, The (R_p) of all types of brasses were exposed to sandy soil with varying moisture levels (Figure 7). The corrosion resistance of all types of brass has been reduced to a maximum of 30% moisture, and then tends to increase when the moisture content exceeds 30%.

As noted in his article, Tomashov [36] has confirmed the existence of a critical point in soil humidity, an increase of moisture content beyond this value promotes a decrease in the soil corrosion activity. But, this controversial point is a changed value and can differ from soil to soil and from metal to another one.

However, Mamedov [37] and Gupta [38] found that underground corrosion was greatest in soils with a moisture content of 25 to 30%, a value quite close to the results obtained. Therefore, in order to know the influence of the elements of addition on the brass corrosion resistance, their roles were discussed as follows:

The influence of the addition of As, Fe and Ni in the brasses, under investigation, on corrosion resistance was studied in sandy soil using EIS. Figure 5 shows the variation of the polarization resistance as a function of the percentage of the elements studied. While, Figure 6 shows the variation of the film resistance as a function of the percentage of Sn and Pb.

We can conclude from Figure 5.a that, the arsenic presence in the brass chemical composition decreases the corrosion rate and increases the brass resistance corrosion. Thus, increasing the As content leads to an increase in R_p value.

Many authors [10, 39, 40] had found that a small quantity of arsenic inhibited the preferential dissolution of zinc from the all alpha brasses. In addition Hollomon and Wulff [41] proved that the minimum corrosion rate is obtained after adding 0.084% of arsenic which is the case of EC3 alloy.

From Figure 5.b, it can be deduced that the presence of Iron in the chemical composition of brass increases the corrosion rate. Moreover, the presence of Fe in the chemical composition leads to accelerate the dezincification rate. According to [10, 42], a small percentage of Fe is responsible of accelerating dezincification brass. They also discovered that manganese similarly fastens dezincification in both types of brasses : α brass and $\alpha+\beta$ brass, even if at a lower rate than iron. For this investigation we confirmed that the EC3 is the more resistant due to the lower percentage of iron and manganese.

From Fig.5c, we can notice that the Nickel presence in the chemical composition of brass increases the corrosion rate, an enhancement rise in Ni content causes the decrease of R_p .

From figure.6a we can conclude that the presence of tin in the chemical composition of studied brasses increases the film resistance. This result is confirmed by Beccaria et al [13], who had proved that Sn forms a passive film on the brass surface.

Other chemists [44] have investigated the influence of Nickel. The Nickel alone hadn't an inhibitive role. A synergistic effect of nickel and tin was found when certain concentrations

were added. With tin concentrations as high as possible of up to 0.7% and 0.5% Ni, the depth of corrosion was reduced.

In addition, from figure 6b, it was found that the film resistance R_f of the studied brasses was increased with the increase in the Pb content, leading to the formation of an insoluble layer of $PbSO_4$. These results explained the decrease in the corrosion rate and the increase of resistance and thickness of the surface film in the presence of Pb (passivation phenomena).

The chemical structures analysis of our samples of $\alpha+\beta$ brass and α -brass, based on the results obtained shows a relationship between the classification of the corrosion resistances and the values of the elements known as determinants of the dezincification phenomenon such as As, Ni, and Fe. This is not the problem of the other elements that confirms the synergistic effect. Thus, it becomes difficult to deduce the element responsible for increasing the resistance or the decrease in the rate of corrosion.

3.2. Dezincification test

The discrepancies in dezincification kinetic of the two alloys EC3 and EC4, are illustrated in Figs. 8 and 9. The comparative experiments in Table 5 show the dezincification depth for the two samples EC 3 and EC4 after 21 days of immersion in a sandy soil of *Essaouira* at 14 % of moisture content.

From table 5, the test of EC 3 shows a better dezincification performance under these conditions comparing to the sample EC 4.

3.3. Influence of chloride contents

Brass devices (α -brass and $\alpha+\beta$ -brass) are used as support fittings, which are suitable for connecting domestic service lines in coastal area i.e. *Essouira* and can be affected by seawater intrusion. Seawater intrusion may lead to the corrosion of underground plumbing devices because of high chloride concentrations. This part is an attempt to enlighten the effect of chloride contents on the corrosion behavior of two brass types by using various electrochemical methods such as spectroscopy of electrochemical impedance or potentiodynamic polarization.

3.3.1. Electrochemical Impedance Spectroscopy (EIS)

The original soil sample (S1) was modified by adding 2% of NaCl dissolved in demineralized water and the corresponding soil was named (S5). The volume of the obtained solution is

appended to the measured dried soil that was calculated to give a relative humidity (RH) of 14% by using a specific electrochemical cell, which is represented in fig.2. The Fig.10 shows the impedance diagrams recorded under open-circuit conditions after 21 days of the $\alpha+\beta$ brass and α -brass immersion in the soil sample (S5).

Impedance diagrams of all brasses under investigation at their corrosion potential were presented in Fig. 10, the same loop obtained in (fig.3 a) is related to the investigated loop for the mechanism of corrosion in chloride surface[44]. The impedance diagrams consist of two loops which are noticeable relatively well separated, at increased frequencies : the first loop might be attributed to the corrosion product film shaped by adsorption, also from heterogeneities within at the surface, and the second at the low frequencies may be assigned to the relaxation of the double layer which is in the same direction with the charge device resistance.

It can be seen from table 6 that the R_p values, corresponding to both of brass types in the studied soil, respect the following order: EC3 > EC4 > EC2 > EC1.

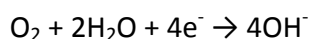
EC3 is always the most resistant among the other alloy even in a very aggressive environment containing the chloride ions. Additionally, the brass EC4 becomes more resistant in comparison with the previous study, related to the influence of moisture content, this could be elucidated as follows:

- Brass with two-phase α and β is less resistant to corrosion than single phase α -brass[45].
- The addition of Zinc changes the corrosion resistance. As a result, when the zinc content becomes higher, the brasses will be sensitive to dezincification processes in chloride solution[46, 47].
- The galvanic couplings that take place in the brass, which has a multiphase ($\alpha+\beta$) and contains 2 % of plumb mass (the case of EC2 and EC1), would accelerate the corrosion process if α and β corrosion potentials are different. Some non-uniform corrosion types can have an effect on the performance of some systems.

3.3.2. Potentiodynamic measurements

In order to investigate the studied alloys (brass devices), the polarization behavior of samples has been compared. Fig. 11 has represented the cathodic and anodic polarization curves corresponding to EC1, EC3, EC4 and EC2 after 21 days of immersion in the soil sample (S5).

The four anodic curves where $\log(i)$ was linked to E have a very similar slope. It seems that polarization behavior of these Cu alloys in chloride solutions is dominated by the copper dissolution to soluble cuprous chloride ion complex (CuCl_2^-)[48]. From the anodic curve, a limiting-current behavior was obtained, this kinetic is justified when the anodic reaction rate was controlled by the formation and dissolution of a CuCl film[49]. In general, the corrosion of Cu alloys, in neutral chloride solutions, involves the cathodic reduction of oxygen:



In the anodic region, the dissolution of copper-zinc alloy in the medium containing the chloride ions generates the following steps:

-First: spontaneous dissolution of zinc, zinc oxide formation and copper oxide Cu_2O formation:



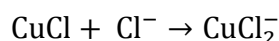
When the surface is covered with Cu_2O and ZnO , CuCl is then formed on the surface according to the reaction:



CuCl can be transformed into CuCl_2 according to the reaction [50-52]:



Also, it can be dissolved with the formation of CuCl_2^- complex via [50-52]:



3.3.3. Characterization of corrosion layers by SEM-EDS analysis:

3.3.3.1. At 14% of moisture content

SEM and EDS analyses were used to define the chemical composition of the corrosion products formed on the brass surface and the morphology of the surface attack. Fig. 12 and 13 give the corresponding SEM images and EDS of all brasses under investigation after 130 days of immersion in sandy soil at 14% of moisture content (fig.12) and in the modified soil (S5) at the same moisture content (fig.13).

The observation of EC4 (Fig.12d) surface has shown that corrosion layer is less compact and uniform, the surface has more crevices and a great number of pits are spotted on it in comparison with EC3 (Fig.12a) ,EC2 (Fig.12b) and EC1 (Fig.12c). Moreover, the porous structure and the presence of the crevices and the pits in the corrosion layer (fig 12c and 12d) produce paths that make the diffusion, of corrosive medium elements (water, oxygen, salt ions and other corrosive media) through metal substrate, easier.

The EDS analysis of the corrosion products formed (presented in table 7) on the EC1 surface reveals the presence of copper and zinc with small amount of oxygen which explains the presence of Cu and Zn oxides. Also the lower percentage of oxygen was found in comparison with other brasses, this observation was attributed to the weak brass dissolution after the immersion in soil medium. The higher Sn content on the surface (comparing with other brasses) indicates that Sn is accumulated at the corrosion product/metal interface, then it forms a passive film which increases the resistance of brass to generalized corrosion [13].

With respect to the EDS data, EC4 and EC1 contain lead, iron and Magnesium with a large amount leading to surface degradation and consequently the corrosion rate becomes greater.

3.3.3.2. At 14% moisture content and with 2% NaCl

The surface morphology of the different studied brasses after 130 days of immersion in an aggressive sandy soil sample (S5) at 14% of moisture content was investigated by SEM. The SEM micrographs for the EC3, EC2, EC1 and EC4 alloys are presented in Fig. 13 a, b, c and d respectively. Spot analysis of the intact surface using energy dispersive X-ray analysis (EDS) have shown the presence of peaks of the component elements of brass, as shown in table 8.

Fig. 13 illustrates the SEM images from brasses sample buried in soil samples (S5) of quite high chloride concentration (2% equal to 2000 ppm), under the same conditions. The morphology of the attacked brass surfaces corresponding to long exposures (130 days) and high chloride concentrations, particularly EC1 and EC2 ($\alpha+\beta$ brass), reveals the peeling of the surface layer (cracked layers). On the other hand, the SEM image corresponding to EC3 and EC4 (α -brass) shows a uniform distribution of a high amount of corrosion, in other words the film seems to be more compact and thicker on the surface.

As can be seen from EDS microanalysis (table 8), the corrosive layer of EC1 and EC2 contains a higher percentage of copper and zinc when compared to EC3 and EC4. The higher percentage of Cu and Zn, which was diffused into the corrosion layer because of Cu and Zn dissolution tendency into the corrosion layer. Also, the higher percentage of O suggests that thicker copper and zinc oxides films have been formed during the corrosion process under the form (Cu_2O , CuO and ZnO) [53]. The presence of Cl^- in the corrosion products indicates the formation of the passive salt layer that covers the surface (CuCl , ZnCl_2) [54]. Moreover, Soil elements such as Fe, Si, Ca, S, Na, Mg, and K are detected in the corrosion products.

The higher Sn content on the surface of EC3 (in comparison with other brasses) indicates that Sn was accumulated at the corrosion product/metal interface then formed a passive film which increases the resistance of brass to generalized corrosion.

The presence of Al, Ni, As, Pb and Fe (additional element in brass compositions) on the surface of corrosion product approves the surface degradation and consequently that the corrosion rate has become greater. The results obtained by EDS and scanning electron microscopy agree with those of the polarization and impedance measurements.

4. Conclusion

Polarization curves and EIS were associated with SEM and EDS techniques to examine the corrosion behavior of two series of brass alloys (brass devices) in sandy soil of Essaouira. The main conclusions can be cited as follows:

- The increasing of moisture content decreases the (R_s) value for the studied soil.
- The corrosion resistance of all types of brass has been reduced to a maximum of 30% moisture, and then tends to increase when the moisture content exceeds 30%.
- The arsenic presence in the brass chemical composition decreases the corrosion rate and increases the brass corrosion resistance.
- The presence of Iron in the chemical composition of brass increases the corrosion rate.
- The Nickel presence in the chemical composition of brass increases the rate of corrosion.

- According to all the moisture content values, the (R_p) values of the both α -brass and ($\alpha+\beta$) brass in the studied soil prove the following order: EC3 > EC2 > EC1 > EC4.
- EC3 is always the most resistant among the other alloys even in a very aggressive environment containing the chloride ions.
- The results which are obtained by *EDS* and scanning electron microscopy agree with those of the polarization and impedance measurements.

Acknowledgement:

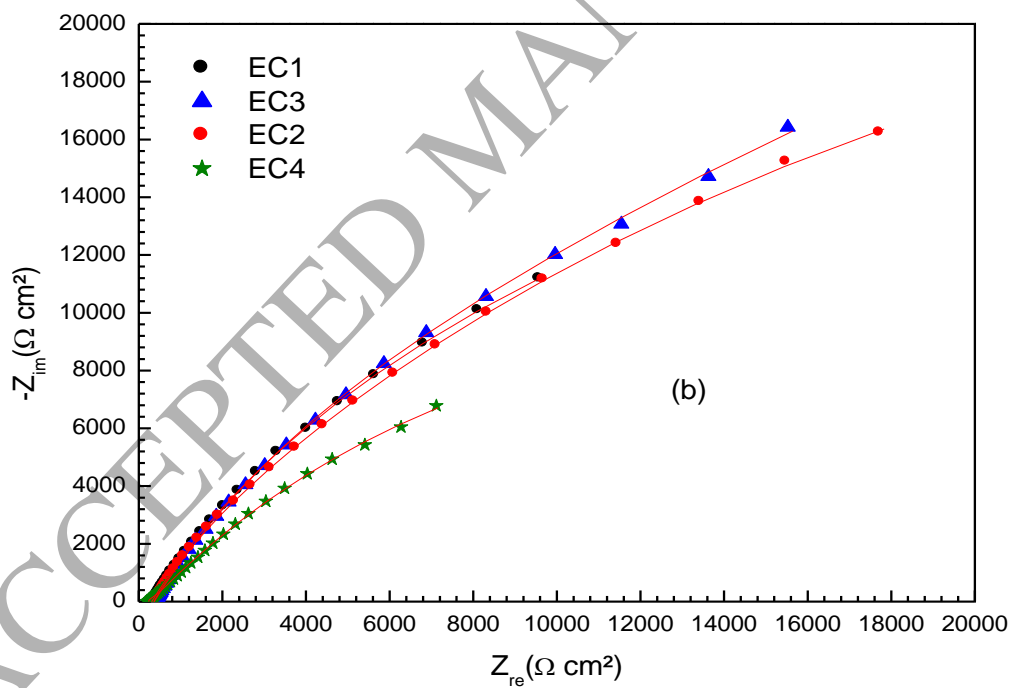
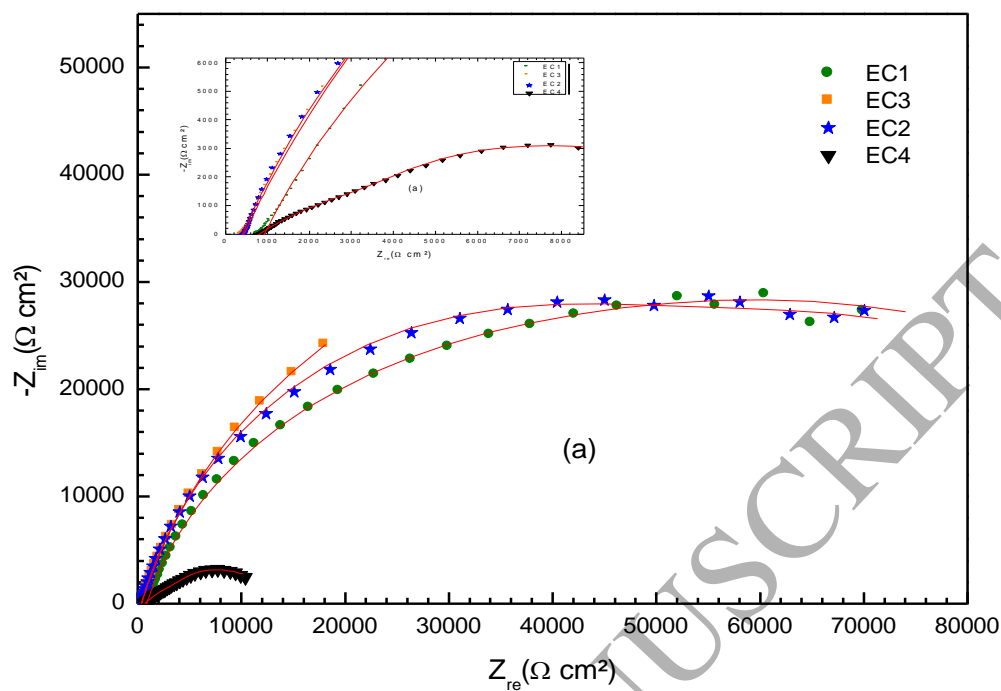
Authors are pleased to acknowledge National office of water and electricity (ONEE), Rabat, Morocco for the financial assistance and facilitation of our study.



Fig.1. Plumbing system examined



Fig.2. Electrochemical system designed for the study of brasses coupons in soil



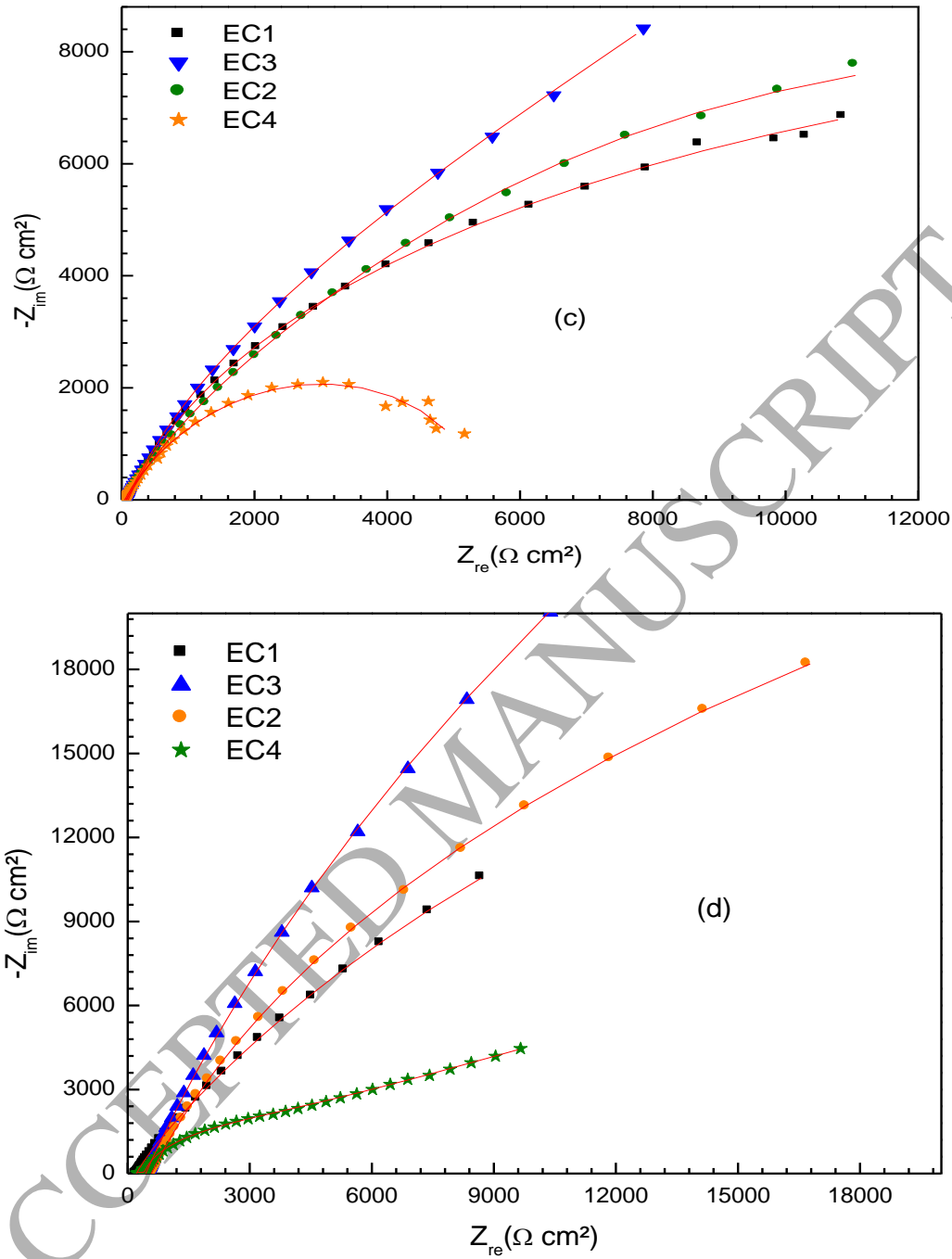


Fig.3. Nyquist plot for four brasses after 21 days of immersion in sandy soil at different moisture contents: (a) 14%, (b) 20%, (c) 30 and (d) 40%.

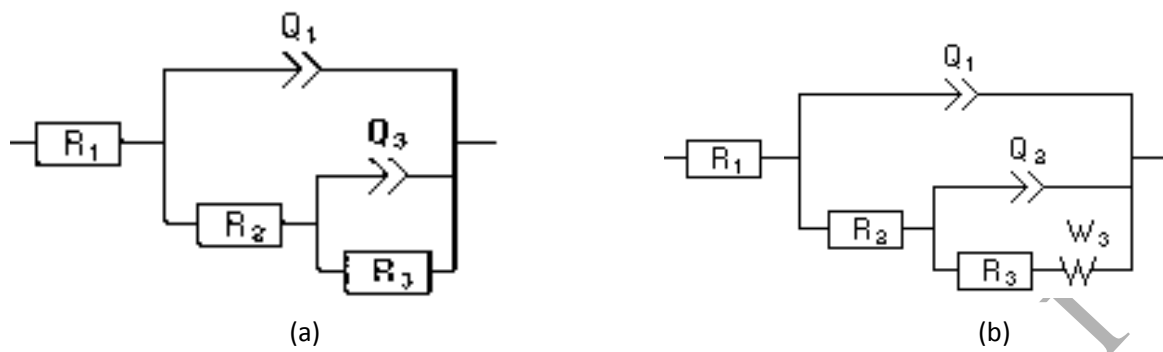
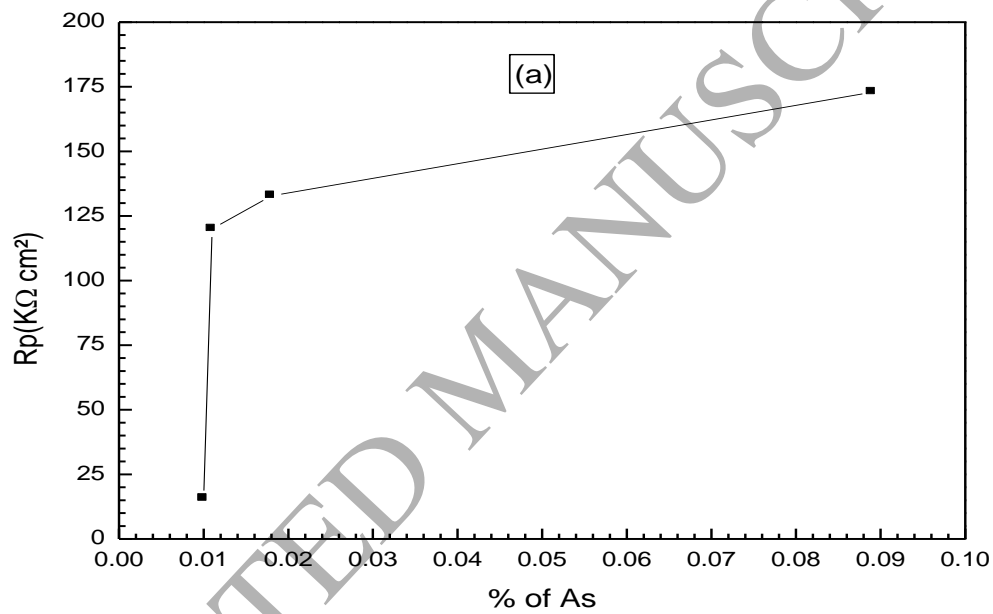


Fig.4. The equivalent circuit model used to fit the experimental impedance data brass devices in a sandy soil at different moisture contents.



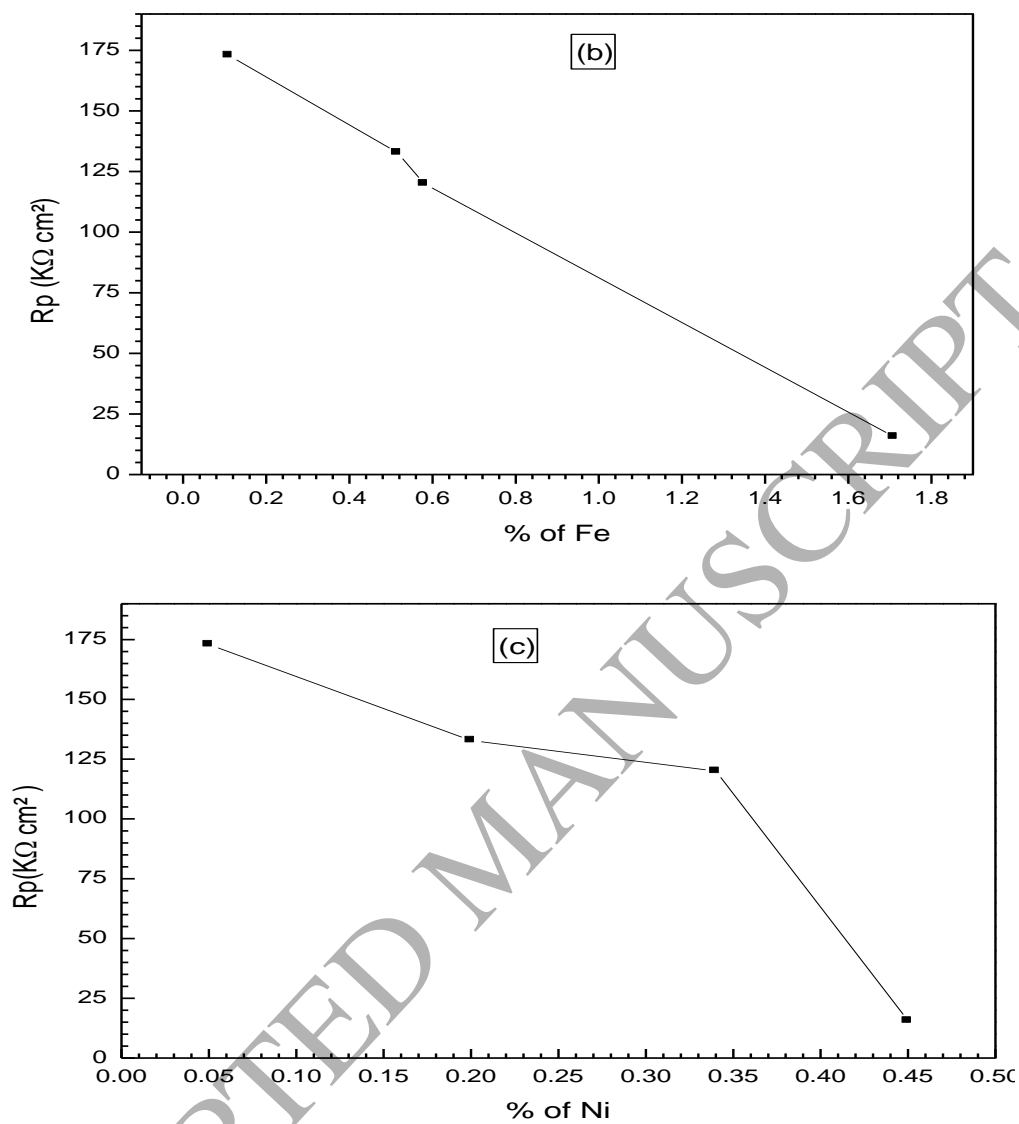


Fig.5. Polarization resistance (R_p) after 21 days of immersion of brass, at 25°C, as a function of (a) the As content. (b) the Fe content. (c) the Ni content.

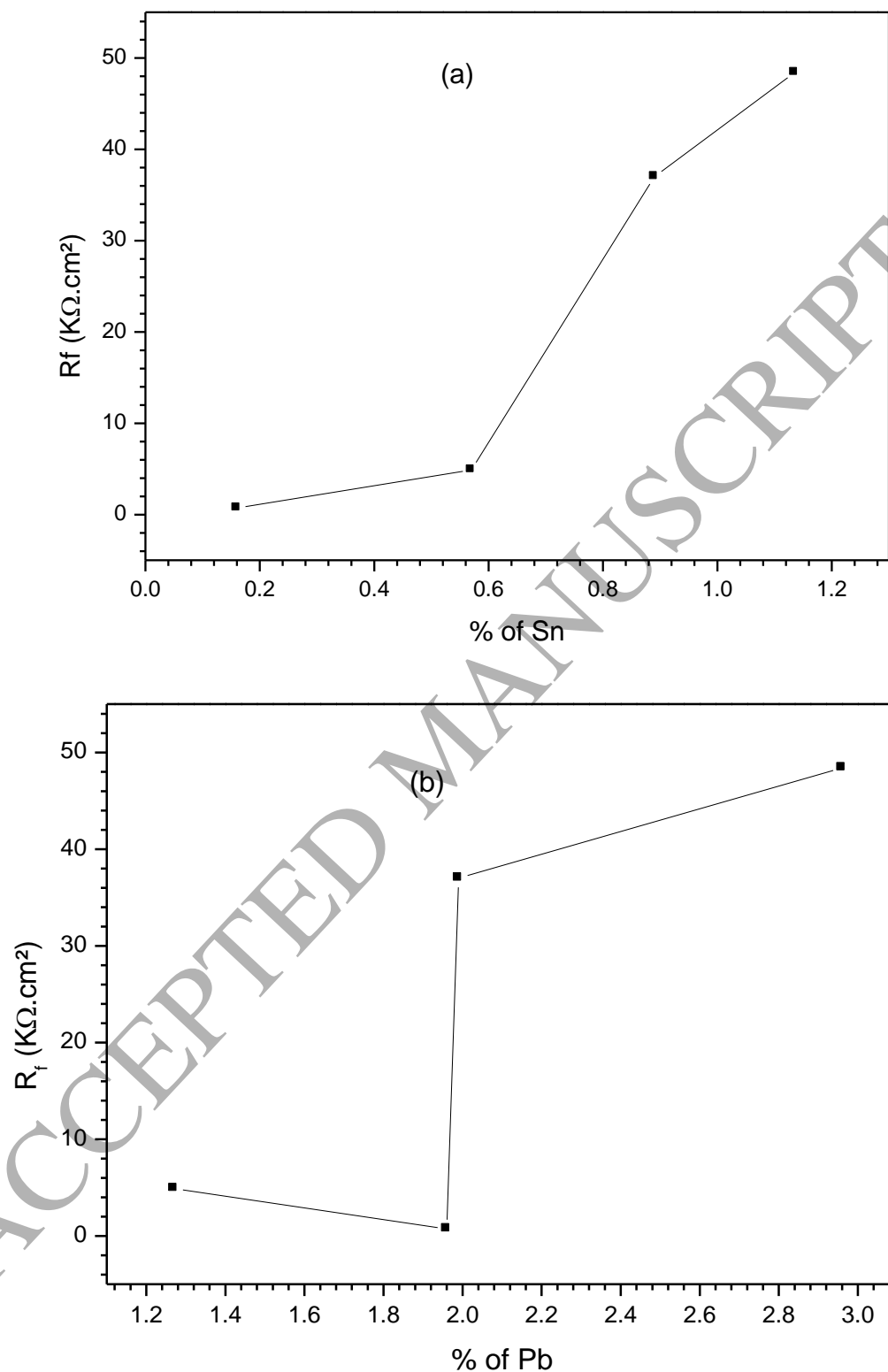


Fig.6. corrosion film resistance (R_f) after 21 days of immersion of brass, at 25°C, as a function of (a) the Sn content. (b) the Pb content.

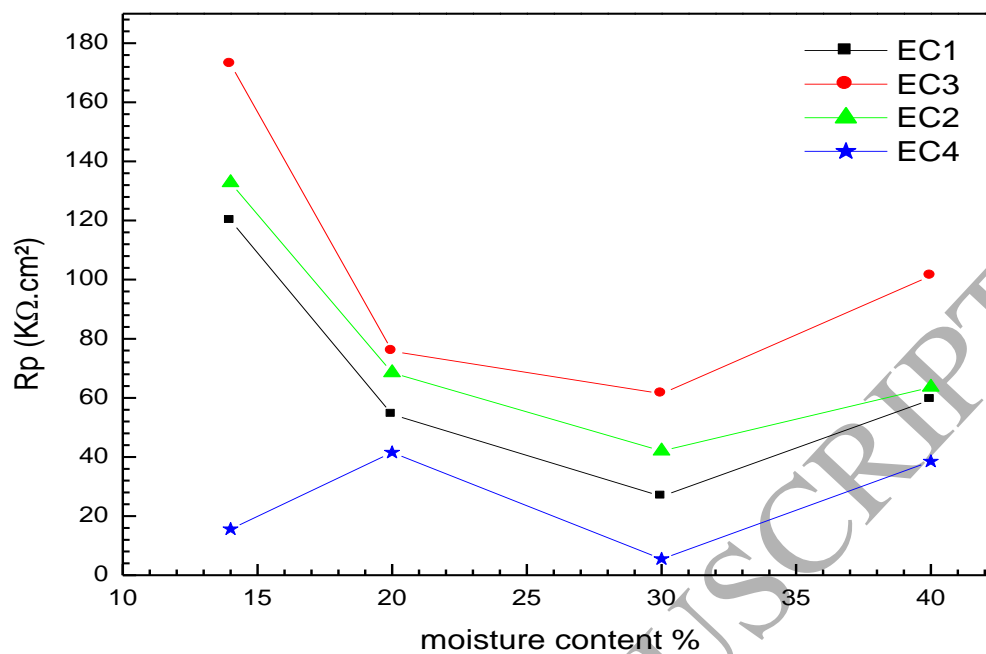


Fig.7. The variation of (R_p) for all brasses types with the moisture content of the studied soil.

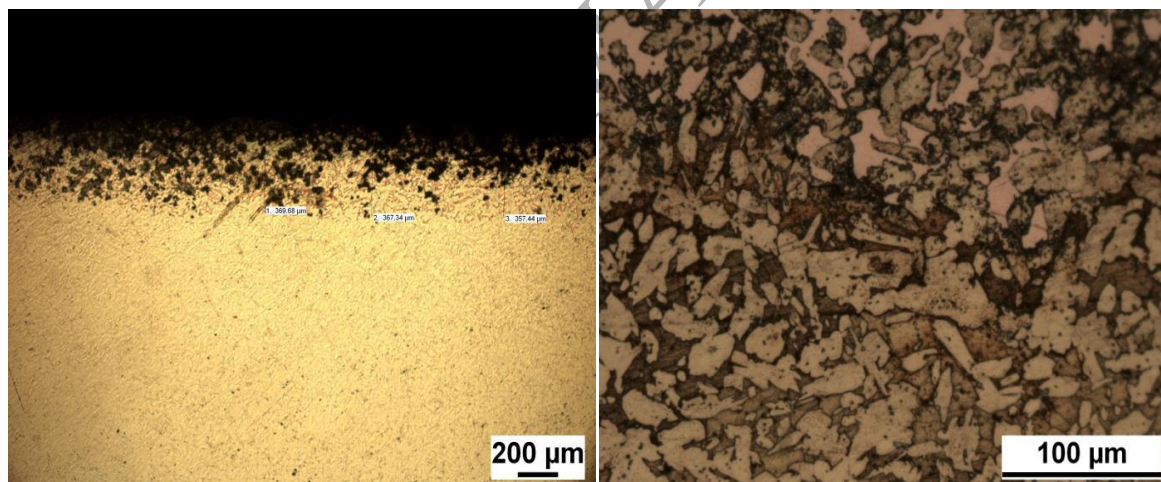


Fig.8. Optical microscope observation of the dezincification structure of sample EC3 after 21 days of immersion in sandy soil of Essaouira at 14 % of moisture content.

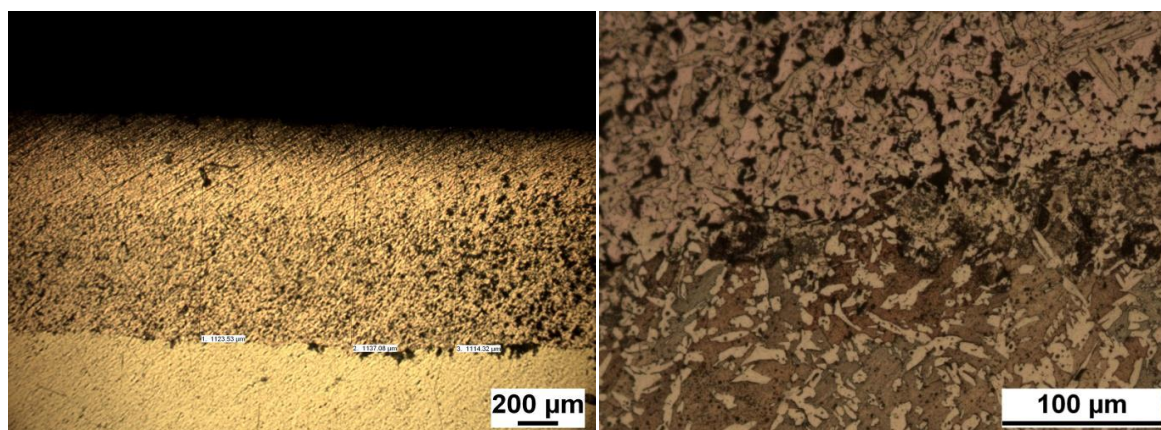


Fig.9. Optical microscope observation of the dezincification structure of sample EC4 after 21 days of immersion in sandy soil of *Essaouira* at 14 % of moisture content

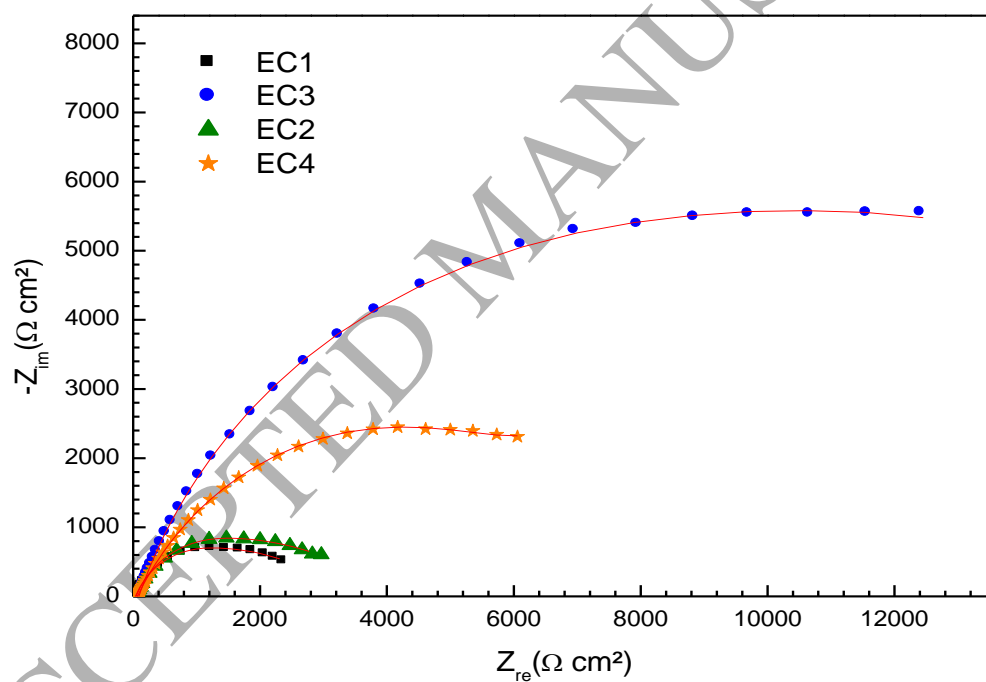


Fig.10. Nyquist plot of all brasses (EC1–EC4) in the soil sample (S5) after 21 days of immersion at 25°C

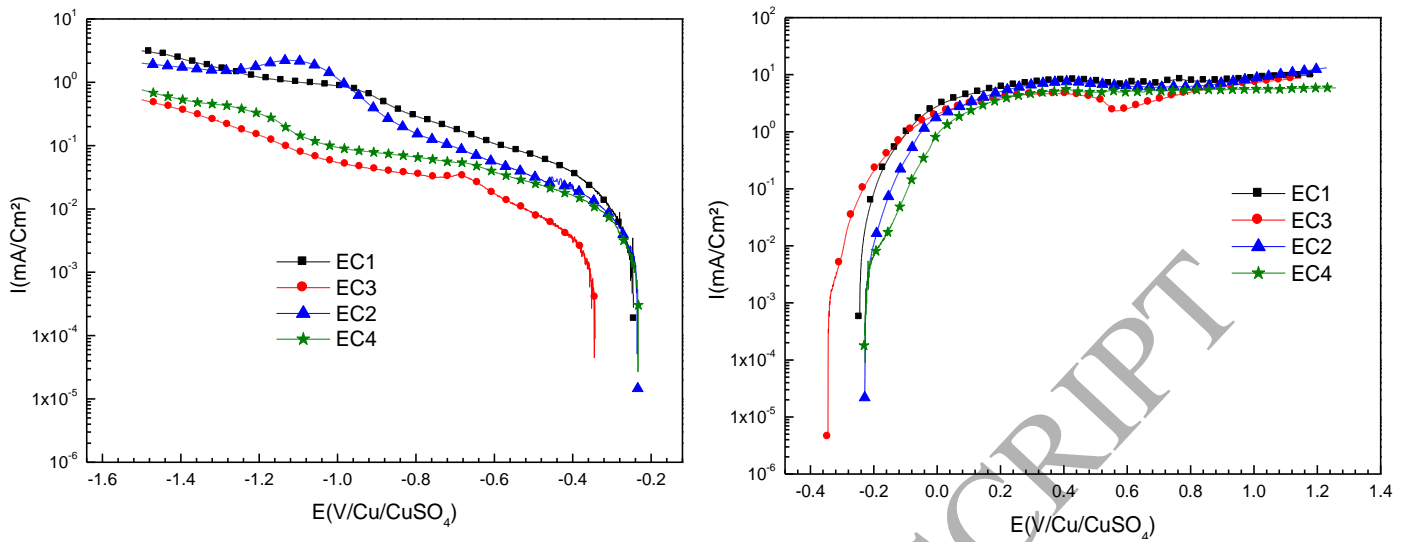
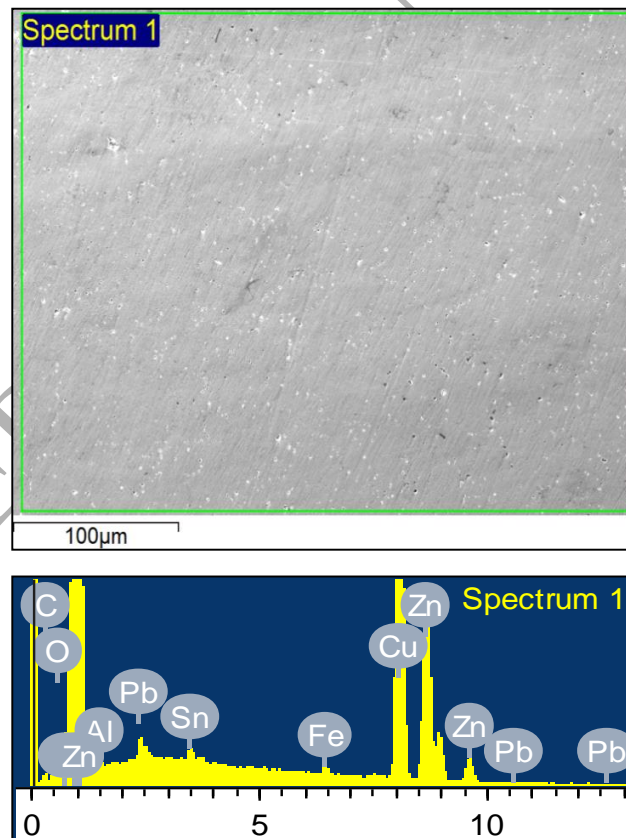
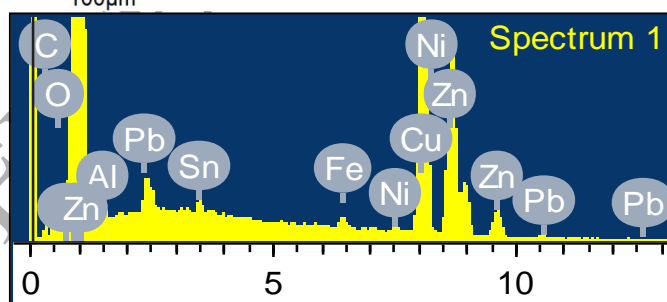
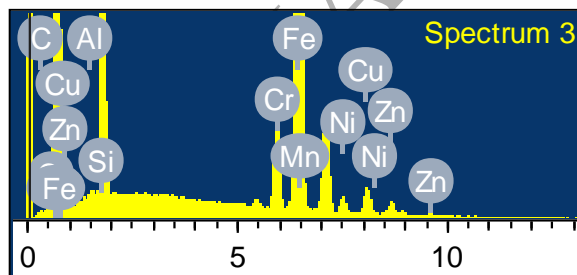
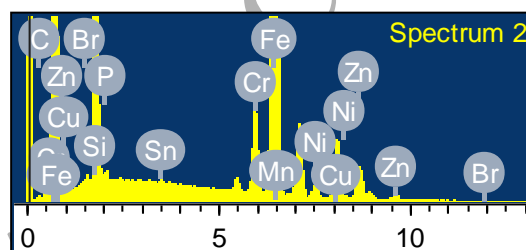
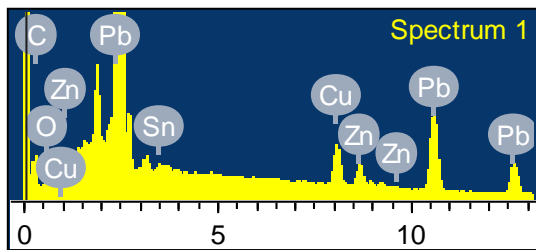
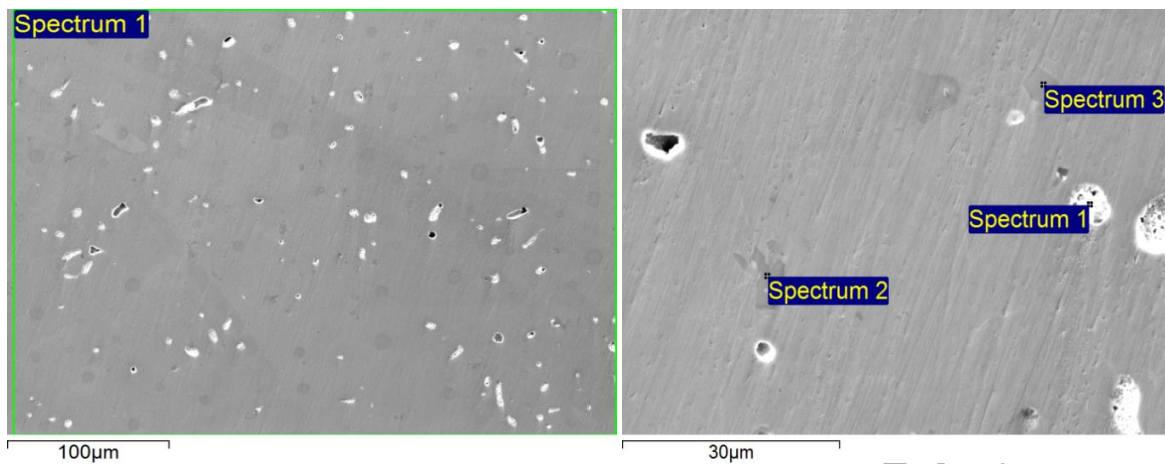


Fig.11. cathodic (a) and anodic (b) Polarization curves for all brasses (EC1–EC4) in the soil sample (S5) after 21 days of immersion at 25°C.

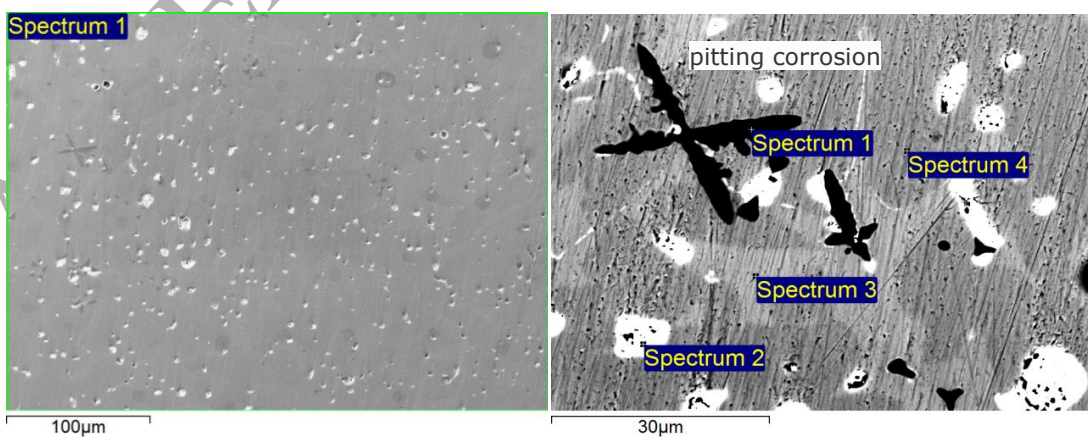


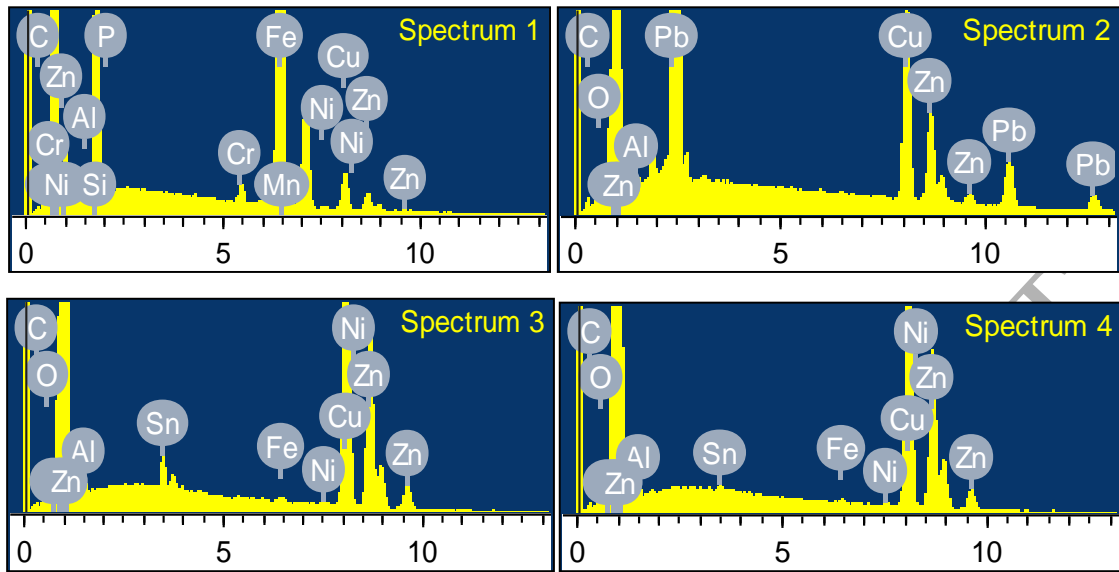
EC3(a)





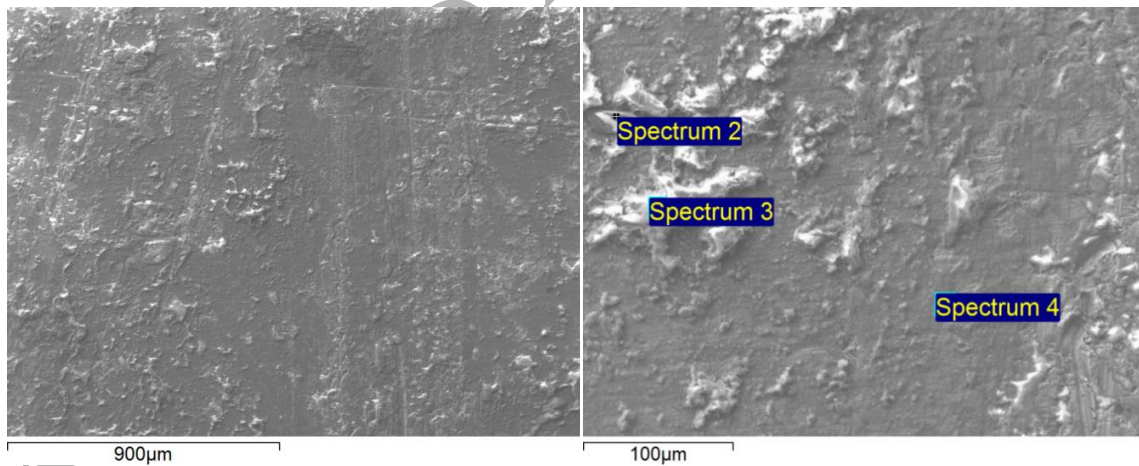
EC1(c)



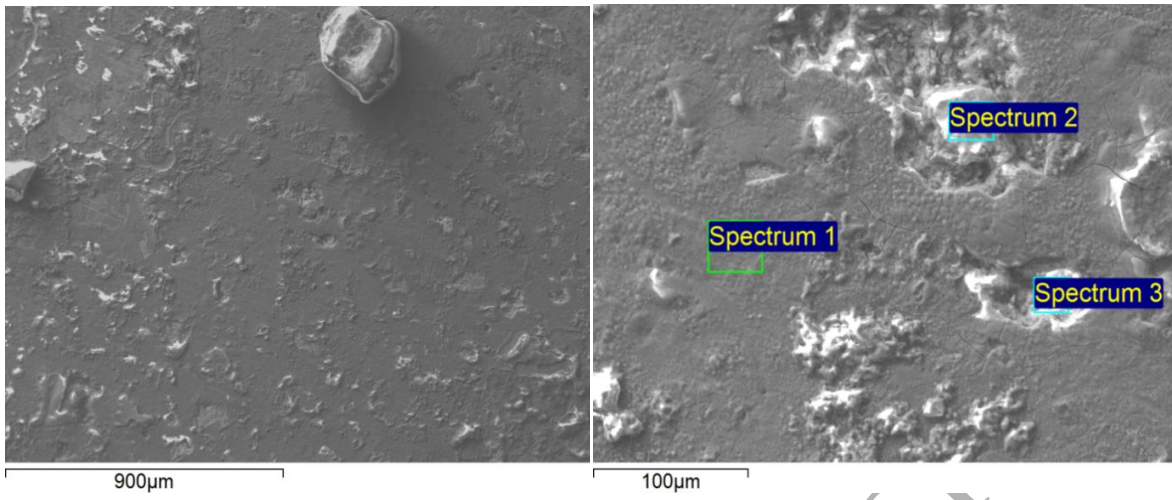


EC4 (d)

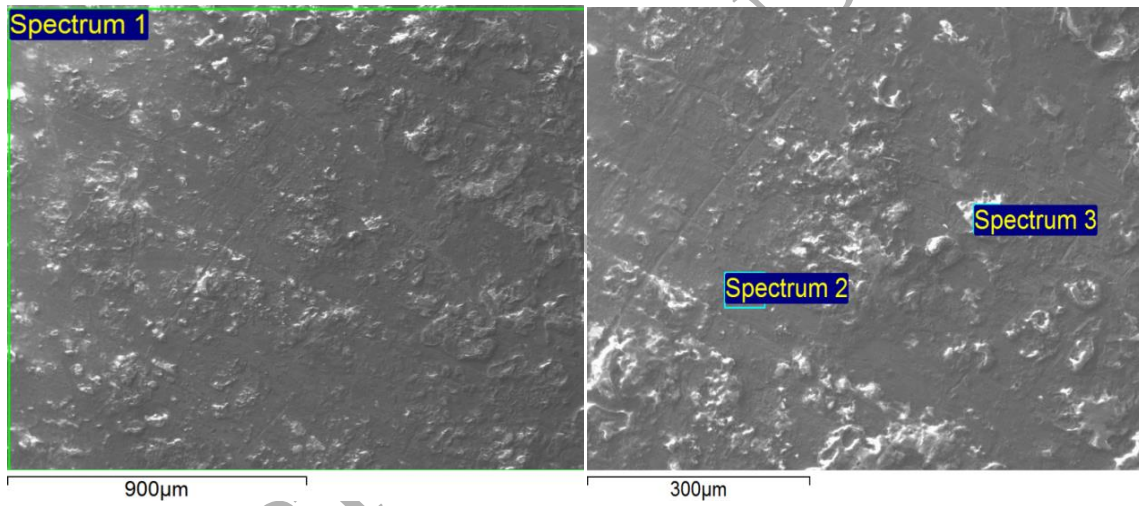
Fig.12. Backscattered electron image (SEM-EDS analysis) of the corroded surface after 130 days of immersion in sandy soil at 14% of moisture content for *all brasses*: EC3 (a), EC2 (b), EC1(c) and EC4 (d).



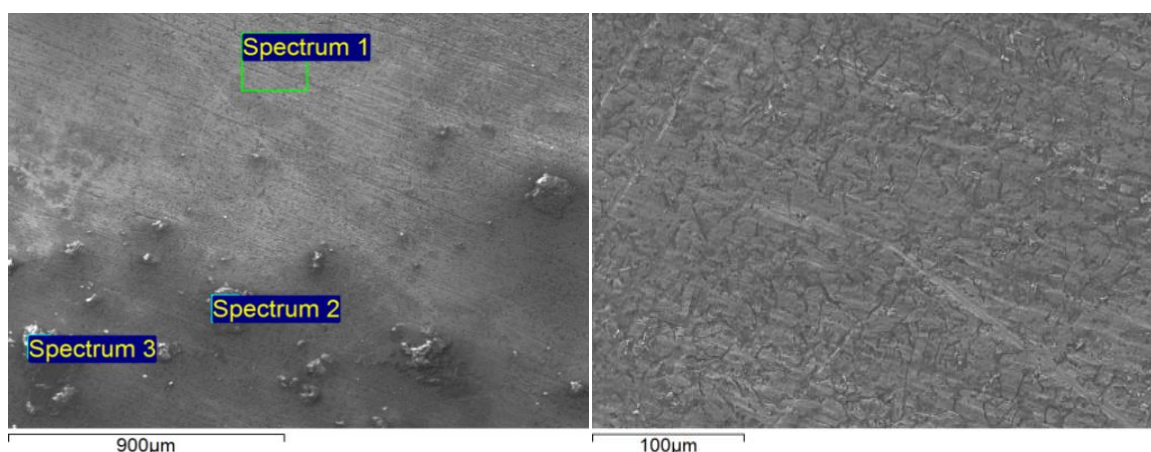
EC3(a)



EC1(c)



EC4(d)



EC2(b)

Fig.13.Secondary electron image (SEM analysis)of the corroded surface after 130 days of immersion in sandy soil sample (S5)at 14% of moisture content for all brasses:EC3 a),EC2 (b), EC1 (c) and EC4 (d).

Table 1Main features of the Essouira soil as received from the field and properties of the soils.

Concentration of various ions in the aqueous extract (mg / l)					
Ca^{2+}	Mg^{2+}	Cl^-	SO_4^{2-}	Na^+	K^+
36	15.6	68.7	61.5	52.67	19.9
Essouira Soil Texture					
Clay	Silt	Sand	pH	Moisture(%wt)	CE(mS/cm)
8.3	13.6	78.1	6,85±0,2	14	0,548

Table 2 Composition of various soil samples

Soil sample	Composition of solution (× : with / - : without)		Moisture content %
	Demineralized water	NaCl (2%)	
S1	×	-	14
S2	×	-	20
S3	×	-	30
S4	×	-	40
S5	×	×	14

Table 3 Chemical compositions of α -brasses and $\alpha+\beta$ brasses with elements of addition

Brass grade	Composition, wt. %												
	α phase	Cu	Zn	Pb	Sn	Fe	Al	Ni	As	Mn	P	Si	Sb
EC1	60.09	57.5	36.85	2.96	1.135	0.58	0.2435	0.34	0.011	0.068	0.00235	0.0595	0.053
EC2	62	58.8	37.14	1.99	0.89	0.515	0.096	0.20	0.018	0.0715	0.004	0.040	0.036
EC3	92.86	62.6	34.91	1.96	0.16	0.11	<0.001	0.05	0.089	<0.0005	<0.0001	<0.0005	0.024
EC4	91.27	70	21.95	1.27	0.57	1.71	3.675	0.45	0.010	0.1365	0.00165	0.0345	0.03

Table 4 Electrochemical impedance parameters of all brasses in the sandy soil with different moisture contents.

TH %	Material	R_s $\Omega.cm^2$	Q_f $\mu F/cm^2$	n_f	R_f $K\Omega.cm^2$	Q_l $\mu F/cm^2$	n_l	R_{ct} $K\Omega.cm^2$	$S3$ $Ohm.s^{1/2}$	R_p
14	EC2	326	25	0.85	37	44	0.6	95.5	-	132.8
	EC3	385	256	0.81	0.72	8	0.35	172.6	112	172.9
	EC1	570	21.4	0.80	48.4	62	0.55	72.2	-	120
	EC4	296	144	0.71	4.9	339	0.63	11.4	-	15.6
20	EC2	308	902	0.99	21.7	210	0.74	47.2	46	68.5
	EC3	315	132	0.77	16.9	90	0.55	59.3	116	75.8
	EC1	309	698	0.64	24.42	308	0.74	30.3	26.2	54.4
	EC4	225	277	1	0.193	316	0.62	41.5	848	41.5
30	EC2	63	445	0.9	8.1	268	0.7	34.5	472.4	42
	EC3	75.5	164	0.78	12.7	192	0.6	49.5	125	61.4
	EC1	78	268	1	4.3	120	0.78	22.5	129	26.7
	EC4	45	390	0.75	2.2	398	0.74	3.8	-	5.5
40	EC2	581	121	0.79	15.24	267	0.98	49	140	63.6
	EC3	444	399	0.54	0.94	271	0.81	100.8	32	101.3
	EC1	201	332	0.77	7.6	123	0.55	52	200	59.4
	EC4	223	73	0.72	4.5	371	0.5	34.3	38.4	38.5

Table 5 the dezincification depth of two samples EC3 and EC4 after 21 days of immersion in the sandy soil of Essaouira at 14 % of moisture content.

Samples	Dezincification depth (μm)
EC3	381.94
EC4	1115.00

Table 6 Electrochemical impedance parameters for all brasses after 21 days of immersion in the soil sample S5 at 25°C.

	R_s ($\Omega.cm^2$)	Q_f ($\mu F/cm^2$)	n_f	R_f ($K\Omega.cm^2$)	Q_{dl} ($\mu F/cm^2$)	n_l	R_{ct} ($K\Omega.cm^2$)	R_p ($K\Omega.cm^2$)
EC3	89	1.2	0.72	7.38	195	0.77	13.28	20.57
EC2	48	310	0.98	1.2	139	0.72	2.7	3.9
EC1	46	2.0	0.87	0.95	154	0.74	2.8	3.7
EC4	66	188	0.97	2.7	302	0.7	7.9	10.53

Table 7 The composition of the corrosion layer formed on surface in each brass electrode after 130 days of immersion in the sandy soil at 14% of moisture content

Element	Brass grad / Weight %									
	EC3		EC2		EC1			EC4		
	Spec 1	Spec 1	Spec 1	Spec 2	Spec 3	Spec 1	Spec 2	Spec 3	Spec 4	
C	2.81	3.25	4.04	1.58	1.48	1.56	2.77	1.72	2.02	
Si	-	-	-	14.14	15.13	11.49	-	-	-	
P	-	-	-	0.47	-	0.23	-	-	-	
Cr	-	-	-	0.75	0.45	0.96	-	-	-	
Mn	-	-	-	6.53	6.03	0.25	-	-	-	
O	0.63	0.88	2.08	-	-	-	1.05	0.55	0.65	
F	-	-	-	-	-	-	-	-	1.20	
Al	0.26	0.48	-	-	0.21	0.84	0.23	0.49	0.45	
Fe	0.56	0.75	-	54.52	66.96	72.22	-	0.29	0.23	
Ni	-	-	-	1.95	2.25	0.29	-	0.35	0.31	
Cu	55.75	0.49	5.31	11.51	4.48	6.85	27.27	54.44	61.70	
Zn	36.86	29.90	3.74	7.75	2.66	4.10	15.43	39.27	34.14	
Br	-	-	-	0.38	-	-	-	-	-	
Sn	1.22	0.52	0.47	0.44	-	-	-	2.89	0.50	
Pb	1.90	0.70	84.36	-	-	-	53.25	-	-	

Table 8 The composition of the corrosion layer formed on surface in each brass electrode after 130 days of immersion in the sandy soil sample (S5) at 14% of moisture content

Element	Samples / Weight %												
	EC3				EC2			EC1			EC4		
	Spe 1	Spe 2	Spe 3	Spe 4	Spe 1	Spe 2	Spe 3	Spe 1	Spe 2	Spe 3	Spe 1	Spe 2	Spe 3
C	5.60	-	-	-	8.50	8.00	8.32	4.59	3.37	2.85	14.91	12.05	11.56
O	34.64	34.81	38.15	32.64	13.69	43.80	46.75	43.53	42.54	36.52	33.41	23.74	35.33
Na	3.47	0.33	3.57	2.77	1.87	1.29	1.36	-	-	-	4.08	3.65	6.32
Mg	1.33	1.04	0.83	0.26	-	-	-	0.75	0.25	0.54	0.24	0.25	-
Al	0.95	4.49	1.27	0.50	4.07	8.14	10.19	0.67	0.58	0.33	0.35	-	0.16

Si	5.77	19.75	2.40	1.23	0.60	0.50	0.48	4.65	0.90	1.08	0.98	0.64	0.41
P	0.12	-	0.18	-	-	-	-	-	0.29	-	0.07	-	-
S	0.48	-	0.43	0.63	0.19	2.18	3.07	0.15	0.41	0.19	0.78	0.11	3.44
Cl	0.74	-	1.79	0.48	0.19	3.36	1.19	3.00	3.22	3.17	1.09	0.28	3.36
K	0.17	6.65	0.35	-	-	-	-	0.28	0.12	-	0.10	-	0.08
Ca	2.98	-	4.57	3.38	-	0.14	0.25	3.33	5.28	1.05	1.45	0.63	0.29
Ti	-	0.36	-	-	-	-	-	-	0.10	-	-	-	-
Mn	0.10	-	-	-	-	-	-	-	-	-	-	-	-
Fe	0.76	0.98	0.55	0.39	2.35	3.89	2.92	0.73	0.27	0.27	0.25	0.16	0.21
Ni	1.25	-	-	-	0.44	0.40	0.46	-	-	-	-	-	-
Cu	17.29	20.84	20.00	21.29	52.42	15.76	12.18	20.68	21.55	18.51	11.90	30.24	3.59
Zn	20.38	10.74	25.29	33.04	15.69	11.24	11.63	17.01	20.48	34.28	28.99	27.62	32.05
Sn	2.96	-	0.60	2.37	-	1.30	1.20	0.27	0.36	0.48	-	-	-
Ba	-	-	-	-	-	-	-	0.30	-	-	-	-	-
As	-	-	-	-	-	-	-	-	-	-	-	-	0.18
Pb	-	-	-	-	-	-	-	-	0.28	0.72	1.39	0.63	2.74

References

- [1] M. Ruhland, *Met. Finish.* 98 (2000) 458.
- [2] C.A. Loto, R.T. Loto, *Int. J. Electrochem. Sci.* 7 (2012) 12021 – 12033.
- [3] D.D. Davies, A note on the dezincification of brass and the inhibiting effect of elemental additions. New York: Copper Development Association Inc. (1993) 1-9.
- [4] N.W. Polan, in: *Corrosion, 9th Edition, Metals Handbook*, ASTM International, Metals Park, Ohio. 13 (1987) 614
- [5] M. Hansen, K. Anderko, H.W. Salzberg, *Constitution of Binary Alloys*, *Journal of the Electrochemical Society.* 105 (1958) 260-261.
- [6] J.E. Bowers, P.W.R. Oseland, G.C. Davies, *Br. Corrosion J.* 13 (1978) 177.
- [7] I. Ogilvie, *Corrosion Coatings South Africa.* 9 (1982).
- [8] R.C. Newman, T. Shahrabi, K. Sieradzki, *Corrosion Sci.* 28 (1988) 873.
- [9] J.Y. Zou, D.H. W, W.C. Qiu, *Electrochim. Acta.* 42 (1997) 1733.
- [10] G.D. Bengough, R. May, *J. Instrum. Met.* 32 (1924) 81.
- [11] R.O. Toivanen, J. Hirvonen, V.K. Lindroos, *Nucl. Instrum. Meth. Phys. Res.* 7 (1985) 200-204.
- [12] C. Fiaud, S. Bensarsa, I. Demesy, M. Tzinmann, *Br. Corrosion J.* 22 (1987) 109
- [13] A.M. Beccaria, G. Poggi, G. Capannelli, The effect on the behavior of α -brasses in sea water of the addition of Al and Sn, *Corrosion Prev. Control.* 10 (1989) 169.
- [14] K. Tronner, A.G. Nord and G.Ch. Borg, corrosion of archaeological bronze artefacts in acidic soil, *Water, Air and Soil Pollution.* 85 (1995) 2725-2730.
- [15] R.F. Tylecote, *J. Archaeol. Sci.* 6 (1979) 345 – 368.
- [16] W. Gerwin, R. Baumhauer, *Geoderma.* 96 (2000) 63–80.
- [17] D.A. Jones. *Principles and prevention of corrosion*, 2nd edn. Prentice Hall, Upper Saddle River, NJ. 1992

- [18] A. Srivastava, R. Balasubramaniam. *Mater. Charact.* 55 (2005) 127–135.
- [19] F.S. Afonso, MSc Thesis, University of Lisboa, Portugal, 2008.
- [20] F.S. Afonso, M.M.M. Neto, M.H. Mendonça, G. Pimenta, L. Proença, and I.T.E. Fonseca, *J. Solid State Electrochem.* 13 (2009) 1757–1765.
- [21] E. López, A. Osella, L. Martino, Controlled experiments to study corrosion effects due to external varying fields in embedded pipelines. *corrosion Science.* 48 (2006) 389-403.
- [22] N. Souissi, *Surf. Eng. Appl. Electrochem.* 49 (2013) 73–77.
- [23] N. Souissi, and E. Triki, *Mater. Corros.* 61 (2010) 695–701.
- [24] L. Moucheng, L. Haichao, C. Chu'nan, *Corros. Sci. Prot. Technol.* 12(2000)219–221.
- [25] W. Yuan-Hui, S. Cheng, Z. Shu-Quan, C. Duo-Chang, L. Guo-Hua, L. Xia, *Corros. Sci. Prot. Technol.* 17 (2005) 87–90.
- [26] F. Xiao-dan, L. Ming-qi, X. Hong-mei, L. Yong-qiang, C. Duochang, *Corros. Sci. Prot. Technol.* 19 (2007) 35–37.
- [27] X. Nie, X. Li, C. Du, Y. Huang, H. Du, *J. Raman Spectrosc.* 40(2009) 76–79.
- [28] Institut National de la Recherche Agronomique (INRA), rabat, Maroc
- [29] M. Barbalat, L. Lanarde, D. Caron, M. Meyerb, J. Vittonato, F. Castillon, S. Fontaine, *Ph. Refait Ph. Corros. Sc.* 55 (2012) 246-253.
- [30] A. Bouckamp, *Users Manual Equivalent Circuit ver. 4* (1993) 51.
- [31] A.M. Abdel-Gaber, B.A. Abd-El-Nabey, M. Saadawy. *Corros. Sci.* 51 (2009) 1038–1042
- [32] C.N. Cao, J.Q. Zhang, *Introduction to the Electrochemical Impedance Spectra*, Science Press, Beijing, (2002).
- [33] H. Robain, C. Camerlynck, G. Bellier, A. Tabbagh, *Geophys. Res. Abstracts.* 5 (2003) 03830
- [34] F. Ozcep, M. Asci, O. Tezel, T. Yas, N. Alpaslan, D. Gundogdu. *European Geosciences Union General Assembly, Wien.* (2005).
- [35] A. Ehteram Noor, H. Aisha Al-Moubaraki. *Arab J Sci Eng.* DOI 10.1007/s13369-014-1135-2
- [36] N. D. TOMASHOV, *Theory of Corrosion and Protection of Metals: The Science of Corrosion.* McMillan, New York. (1966).
- [37] A. Mamedov, *Izv. Ak. Nank. Azerbuidchan S.S.R. Serv. fiz., Tech. Khim. Nank.* 6 (1958) 99.
- [38] S. K. Gupta and B. K. Gupta. *Corrosion Science.* 19 (1979) 171-178.
- [39] F.W. Fink, *Trans. Electrochem. Soc.*, 75 (1939) 441.
- [40] R.W. Sullivan, *INCRA Project No 178*, June (1971), 47.
- [41] J.H. Hollomon, *Met. Wulff, Tech.* 8 (1941) 3; *Trans. AIMME*, (1942) 147-183.
- [42] K. Oishi, T. Tsuji, Y. Watanabe, *Proc. International Symp. on "Corrosion of copper and copper alloys in building"*, Jap. CDA, Tokyo. (1982).
- [43] S. Seungman, T. Kang. *Journal of Alloys and Compounds.* 335 (2002) 281–289.
- [44] H.O. Curkovic, E. Stupnisek-Lisac, H. Takenouti. *Corros. Sci.* 52 (2010) 398.
- [45] B.A. Weidon, *BNFMRA Research Report A1148*, April (1957).

- [46] B.Assouli, (2002) Etude par émission acoustique associée aux méthodes électrochimiques de la corrosion et de la protection de l'alliage cuivre-zinc (60/40) en milieu neutre et alcalin. Thesis, INPT, France.
- [47] K.M. Ismail, R.M. Elsherif, W. A. Badawy. *ElectrochimicaActa* 49 (2004) 5151–5160
- [48] A.M. Alfantazi, T.M. Ahmed, D. Tromans, *Materials and Design*. 30 (2009) 2425–2430.
- [49] D. Tromans, J.C. Silva. *Corrosion*. 53 (1997) 171-8.
- [50] A.L. Bacarella, J.C.Jr. Griess, J. *Electrochem. Soc.* 120 (1973) 459-465
- [51] S.K.Chawla, B.I. Rickett, N. Sankarraman, J.H. Payer, *Corrosion Science*, 33 (1992) 1617-1631.
- [52] W.A. Badawy, F.M. AL Kharafi, *Corrosion*, 55 (1999) 268-277.
- [53] I.T.E. Fonseca, E. Niculita, I. Ornelas, M.D. Carvalho, P.D. Vaz, *Corrosion*.DOI: CJ-1503-OA-1720.R2
- [54] M.A. Almomani, W.R. Tayfour, M.H. Nimrat, *Journal of Alloys and Compounds*. DOI :10.1016/j.jallcom.2016.04.006.

Graphical abstract (optional, however strongly recommended)



ACCEPTED MANUSCRIPT